Polyolefin fiber-reinforced concrete enhanced with steel-hooked fibers in low proportions

M.G. Alberti, A. Enfedaque, J.C. Gálvez , M.F. Cánovas, I.R. Osorio

A B S T R A C T

Over the past few years, polyolefin fiber reinforced self-compacting concrete has shown high performance in both fresh and hardened state. Its fracture behavior for small deformations could be enhanced with a small amount of steel-hooked fibers, obtaining a hybrid fiber-reinforced concrete well suited for structural use. Four types of conventional fiber-reinforced concrete with steel and polyolefin fibers were produced on the basis of the same self-compacting concrete also manufactured as reference. These concrete mixtures were manufactured separately with the same fiber contents being subsequently used for two more hybrid mixtures. Fracture properties, in addition to fresh and mechanical properties, were assessed. The research showed both synergies (with the two types of fibers working together in the fracture processes) and an improvement of the orientation and distribution of the fibers on the fracture surface.

Keywords:
Hybrid fiber-reinforced concrete
Polyolefin fiber-reinforced concrete
Steel fiber-reinforced concrete
Self-compacting concrete and fracture

1. Introduction

Over the past decades one of the most important improvements that has taken place in the building industry has been the appearance of self-compacting concrete (SCC). Its main advantages over a standard concrete involves the ease in which it flows to all parts and chinks of the formwork, the way in which it moves around the reinforcement, the absence of vibration due to its consolidation under its own weight, improved mechanical properties and significant durability [1,2]. All these characteristics both enhance productivity and reduce the overall cost of the structure. Self-compactability is achieved through modifying the proportions of the components of a conventional concrete, such as the amount of cement and proportion of superplasticizer employed. Other components might also be used such as a viscosity modifier chemical admixture and/or a mineral admixture of limestone powder. While these modifications provide an improvement of the mechanical and durability characteristics of the concrete, in most of the cases above the requirements of the structure, they cause an increment in the cost (due to this improvement in strength, most of the published studies deal with high strength SCC [3]). In addition to cost, one other drawback is shrinkage cracking that is a side effect of the large amount of fine particles in the formulation [4].

Once SCC has hardened, there are few differences between this and a standard concrete, with two being that they are quasi-brittle materials with low tensile strength and good compressive strength. Adding small amounts of fibers might not only reduce the previously mentioned problem of shrinkage cracking [5], but also increase mechanical properties such as tensile strength and toughness [6]. The fibers added to the concrete paste while mixing are short elements with a reduced section and randomly distributed. Fibers may be manufactured through using many materials such as steel, palm, glass, carbon, or polypropylene, among others [7,8]. The increment in the mechanical properties of the concrete will depend mainly on the material of the fibers, their geometrical characteristics and the amount of fibers added. In some cases there is such an increment of the mechanical properties that the contribution of the fibers may be taken into account in the structural design [9].

Among the fibers used, the most common are made of steel due to their high modulus of elasticity and tensile strength. Concrete with steel fibers has been widely employed in the building industry for some time in applications such as industrial and airport pavements, reinforcement of projected concrete, and precast elements with reduced thickness, among others [10]. These uses have been based on extensive studies of the mechanical behavior of this type of concrete under tensile stresses, fatigue or even impact [11–13]. However, there are certain applications (such as tunnels and continuous slabs of high-speed railway) in which a concern about the effect of steel fibers on the magnetic and electric fields has led to the quantity of fibers used being reduced. Furthermore, the influence of the corrosion of steel fibers in the durability and performance of concrete remains a matter of study [14–16].

One way of overcoming these problems is by adding several shapes and sizes of fibers made from the same material [17,18]. The synergies that appear through using this option have been previously studied [19]. Another way is adding fibers made from different materials and with dissimilar shapes [20–24]. Some studies have analyzed the synergies that appear when mixing different types of steel and polypropylene fibers [25,26]. In such studies the optimum proportions of fibers are established, as well as the contribution of the fibers to the mechanical properties of the composite material. In addition, the behavior of this material was studied under repeated loading [27]. However, the newest technology in precast factories and for *in situ* applications, together with the improvements in concrete admixtures, enables production of SCC at a more competitive cost. This is achieved by reducing the cement content and by having a minimum amount of super-plasticizer [28], thus promoting the research of modifications of this type of concrete. The conjunction of SCC and fiber-reinforced concrete is one such option. The workability of concrete with a cocktail of steel fibers, the fiber anisotropy and the mechanical and fracture properties have been recently studied [29–32]. Due to the problems previously mentioned, cocktails of synthetic and steel fibers added to SCC are analyzed. Other studies have examined the effect of different proportions and fiber shapes, changes in the workability of the concrete [33], and the respective mechanical properties [34,35]. In addition to these, some have viewed the contribution of two different types of fibers (steel and polypropylene) added to a standard reinforced concrete beam [36]. Nonetheless, almost all of these studies have been performed through using one type of fiber that is not structural, polypropylene fiber, and one fiber that can be considered structural, steel fiber [37].

Over the last few years the development of new synthetic fibers has been boosted with the improved mechanical properties, giving place to a field of new applications [38]. Among synthetic fibers, polyolefin ones are those that have been designed to approximate the post-cracking behavior of a polyolefin fiber-reinforced concrete to a steel fiber-reinforced concrete with lower fiber contents (in terms of weight) [39,40]. These new synthetic fibers provide a two-fold benefit: an alternative when a structural contribution of fibers is needed and use of steel fibers is unwise or inadmissible [41]; and synergies in steel fibers and synthetic structural fibers [42]. One of the possible advantages over steel fibers could be improved performance in fresh state (which should be validated on a SCC). The weak point of synthetic fibers, probably caused by the low modulus of elasticity and the frictional adhesion with matrix, is the reduced load borne at small deformations when compared to a steel fiber-reinforced concrete (SFRC) [43].

At the time of writing, given that a SCC with a cocktail of two types of structural fibers of different nature, polyolefin and steel fibers, is still a matter of study, there are both fresh and hardened characteristics of the concrete that merit analysis. Regarding SCC, there are subjects that might be of interest such as the improvement in self-compactability caused by the substitution of a certain amount of steel fibers for polyolefin ones and changes in the polyolefin fiber orientation that the presence of steel fibers may produce. Concerning the hardened properties, there are no analyses of the behavior of a self-compacting hybrid fiber-reinforced concrete performed with polyolefin and steel fibers under tensile or compressive stresses. Furthermore, it could be of significant interest to study the fracture properties and toughness of a concrete with a cocktail of polyolefin and steel fibers with the aim of evaluating the possible use in structures instead of a standard reinforced concrete. Another way to focus research could be to improve a polyolefin fiber-reinforced concrete with a small quantity of steel fibers, enhancing the fracture behavior on the very first deformations. With a low amount of short steel-hooked fibers it would be possible to reduce the load drop, due to its mechanical properties and the hooked shape. When they fail, the high deformations already reached would mobilize polyolefin fibers resistance which would bear stresses up to much higher deformations. Additionally, this would allow a total traditional reinforcement substitution.

In order to achieve these objectives, an experimental campaign was performed by adding two amounts of polyolefin fibers, 4.5 and 6 kg/m^3, to a reference SCC. This involved assessment of the fresh state behavior and the hardened and fracture properties, as well as the flexural and toughness improvements that the polyolefin fibers provide to the control SCC. To compare the influence of the types of fibers, two amounts of steel fibers (25.88 and 38.82 kg/m^3) were added to the same control SCC and the fresh and hardened properties studied. To study the synergies between the steel fibers and the new structural synthetic fibers in a SCC, manufacture of a SCC with polyolefin and steel fibers was attempted. This entailed two hybrid fiber-reinforced concretes being manufactured with the following amount of fibers: 25.88 kg/m^3 and 4.5 kg/m^3 of steel and polyolefin fibers respectively and 20 kg/m^3 and 6 kg/m^3 steel and polyolefin fibers respectively. These two hybrid concretes were characterized and their properties compared with those of the SCC reinforced only with one type of fiber.

Given that the contribution of fibers in the fracture process is strongly influenced by their distribution and orientation, if different mechanical behaviors are obtained, they may be explained due to an improved fiber positioning. To analyze this phenomenon a counting exercise was carried out in the fracture surfaces and related to the fracture tests.

2. Materials and mix proportioning

2.1. Materials

For the concrete production a Portland cement type EN 197-1 CEM I 52.5 R-SR 5 and mineral admixture of limestone was used as a micro-aggregate with a specific gravity and Blaine surface of 2700 kg/m^3 and 400–450 m^2/kg respectively. The calcium carbonate content of the limestone powder was higher than 98% and less than 0.05% was retained in a 45 μm sieve. A polycarboxylate based superplasticizer named Sika Viscocrete 5720 with a solid content of 36% and 1090 kg/m^3 density was employed.

As regards the aggregates, the mixtures were made with siliceous aggregates composed of two types of gravel 4–8 mm and 4–12 mm and sand 0–2 mm. The grading curves of the aggregates are shown in Fig. 1 with a maximum aggregate size of 12.7 mm.

Two types of fibers were used: steel-hooked fibers with a smooth surface and 35 mm long, and polyolefin straight fibers with a rough surface and surface treatment and 60 mm long. Table 1 compares the main characteristics of the types of fiber, their material properties and their geometrical patterns.

2.2. Mix proportioning and concrete production

The starting point to perform the concrete mix proportions was to achieve a mixture with moderate cement content able to reach the self-compacting fresh properties required even with the addition of the two types of fibers. In order to do so, a plain SCC with a slump-flow spread target of 650 mm containing 375 kg/m^3 of cement, and with a water-to-cement ratio of 0.50, was previously designed. To obtain the required fresh properties, 1.25% of cement weight of superplasticizer was needed. The optimum distribution of the aggregates was taken as the maximum dry packing density obtained according to the ASTM C29/29 M-09. Thus, the optimum aggregate skeleton was taken as 24%, 16% and 60% of gravel, grit and sand respectively which implied 25.5% of voids. Aggregates

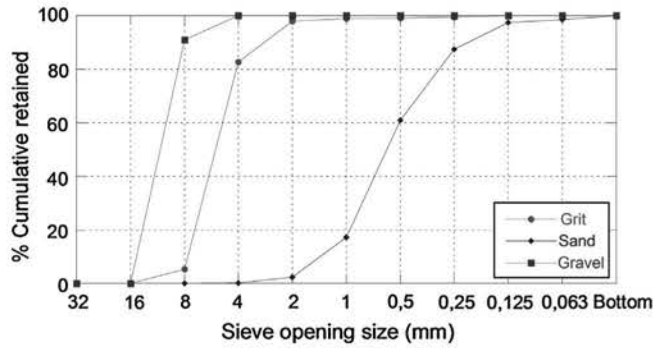

Fig. 1. Grading curves of the aggregates.

humidity was corrected in the first step of the mixing process. The time schedule is shown in Fig. 2.

One plain concrete was manufactured in order to compare the influence of adding fibers and was named REF. To obtain a reasonable value of hybrid fiber proportions added to a SCC, values in the medium and lower threshold of their use were chosen for the two mixtures of steel fibers. However, regarding the polyolefin fiber contents, medium amounts were employed to reach as high a number of fibers as possible in the hybrid concretes. Two fiber contents of two fiber types had to be added to the hybrid FRC to maintain the fresh properties close to the reference SCC, exceeding 1% in volume fraction was avoided. All are summarized in Table 2.

Hence, a volume fraction of fibers of 0.49% was chosen to perform one mixture of both polyolefin and steel fibers separately. In the end, as it allowed a meaningful comparison of fresh and hardened properties a direct evaluation of the fracture behavior of the two types could be carried out. For the SFRC, the volume fraction of 0.33% was also used in order to obtain a result in the lower threshold of their use. In terms of weight, this was equivalent to adding 25.88 kg/m^3 of fibers. In the case of the volume fraction of 0.49%, this represented 38.82 kg/m^3 of steel fibers. In that of polyolefin fibers, the same volume fraction was in terms of weight 4.5 kg/m^3. One more mixture, with 0.66% or 6 kg/m^3, was also manufactured for a subsequent comparison with hybrid mixtures. The two mixtures with steel fibers were called S33 and S49 and the two mixtures with polyolefin fibers called P49 and P66.

The hybrid fiber proportions added to the mix were chosen with the aim of achieving an improved polyolefin fiber reinforced concrete (PFRC) with a small quantity of steel fibers. In that sense, the smaller fraction volume explained above of 0.33% was chosen to evaluate the synergies when a fiber cocktail with a 0.49% volume fraction of polyolefin fibers were added. This hybrid mixture was called H1, with a total fiber volume fraction of 0.82% having a total addition of 30.5 kg/m^3 of fibers.

The research purpose was to produce a FRC with a combined use of both types of fibers that preserved the fresh properties and enhanced the concrete hardened behavior of PFRC with a small amount of steel-hooked fibers. With that aim, one more hybrid mixture was produced in which the quantity of steel fibers was lessened to 20 kg/m^3 (with a corresponding volume fraction of 0.25%) and mixed with up to 6 kg/m^3 of polyolefin fibers completing the mix H2. While it is true that the total fiber volume fraction reached 0.91% (with it being higher than in H1), in terms of weight this entailed a total weight of fibers of 26 kg/m^3 and reduction of 4.5 kg/m^3. Furthermore, it allowed a comparison between two hybrid mixtures.

Based on the plain SCC mix design used as reference (REF), the six FRC mixtures were manufactured. In addition to the mentioned REF, FRC mixtures S33, S49, P49 and P66 were performed with only one type of fibers. Hybrid FRC mixtures H1 and H2 completed the research, as was previously stated, and is shown in Table 2. All were manufactured with a vertical axis concrete-mixer with 100 l of capacity. Nine cylindrical specimens with a diameter of 150 mm and height of 300 mm, and three prismatic specimens of dimension 430 × 100 × 100 mm^3, were produced for each mixture. All the specimens were cured in a climatic chamber (20 °C and 95% humidity) until the age of testing.

3. Tests program and results

3.1. Assessment of fresh state concrete properties

In order to characterize and compare the fresh state behavior of every concrete type, two tests were performed. The slump-flow test described in the standard EN: 12350-8 [44] and the V-funnel test in the standard EN: 12350-9 [45]. The results of both tests on every concrete type are shown in Table 3.

It should be noted that all the results for REF and monotype FRC were among the limits of the most common standards which set a slump-flow spread (d_f) from 550 mm to 850 mm, a time for the slump-flow patty to reach 500 mm of diameter (T_{500}) lower than 8 s, and an emptying time of the V-funnel between four and 25 s [46].

The slump-flow spread mean diameters showed a reduction, as expected and show in Refs. [29] or [32], with the addition of fibers when compared with the results of plain concrete REF. As also anticipated in Ref. [38], steel fibers had more influence on the flow properties with significant reduction of the patty. Times obtained for T_{500} remained at similar values for all the concrete types. In

Table 1
Properties of steel and polyolefin fibers.

Fiber type	PF  Polyolefin fiber	SF 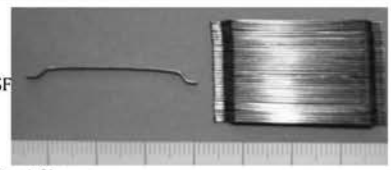 Steel fiber
Fiber shape	Straight	Hooked
Density	0.910 g/cm^3	7.850 g/cm^3
Length	60 mm	35 mm
Eq. diameter	0.903 mm	0.550 mm
Tensile strength	>500 MPa	1100 MPa
Modulus of elasticity	>9 GPa	210 GPa
# Fibers per kg	27,000	14,500
Surface structure	Rough	Smooth

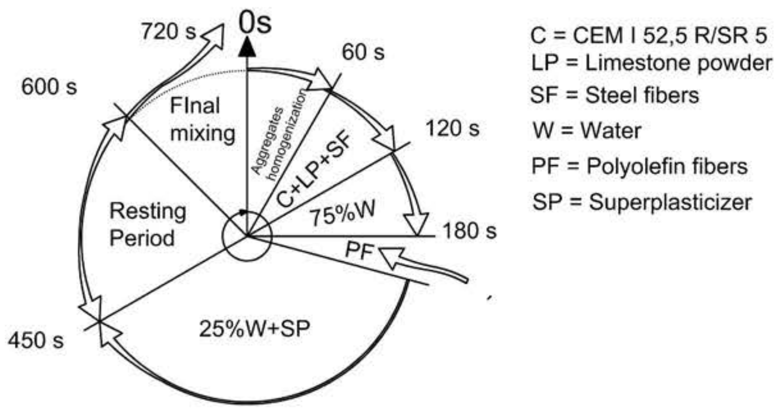

Fig. 2. Mixing sequence.

Table 2
Concrete mix proportions.

Cement (kg/m^3)	Limestone powder (kg/m^3)	Superplasticizer	Water (kg/m^3)	Sand (kg/m^3)	Grit (kg/m^3)	Gravel (kg/m^3)
375	200	1.25% (CEM)	187.5	918	245	367

Mixture	SCC	PFRC		SFRC		Hybrid FRC	
	REF	P49	P66	S33	S49	H1	H2
Steel fibers (kg/m^3)	–	–	–	25.9	38.8	25.9	20
Polyolefin fibers (kg/m^3)	–	4.5	6	–	–	4.5	6

Table 3
Test results for assessment of fresh concrete and mechanical properties.

Concrete	Slump flow test		V-funnel	f_{ck} (MPa)		E (GPa)	f_{ct} (MPa)	
	d_f (mm)	T_{500} (s)	t (s)	28d	c.v.	28d	28d	c.v.
REF	655	3.5	8	39.0	0.01	35.8	3.78	0.14
S33	570	3.5	10	41.7	0.01	33.7	5.32	0.15
S49	570	3.5	14	43.0	0.01	31.9	6.19	0.07
P49	600	3.5	11	38.5	0.06	31.2	4.18	0.20
P66	590	4.0	16	41.4	0.01	31.6	4.09	0.03
H1	565	4.0	14	36.5	0.03	33.0	5.41	0.04
H2	560	4.0	25	36.9	0.02	31.8	5.35	0.08

Fig. 3 the slump-flow spread of the hybrid mixture H1 is portrayed to highlight the uniform distribution of fibers and the aggregates on the spread and also with no segregation signs.

As regards the V-funnel test results, it is important to mention that the hybrid mixtures had significantly higher fiber proportions which led to higher emptying times being obtained. Given that the test measures the fluidity and passing capacity, fiber addition increased the emptying times as the volume fraction rose. According to this, for hybrid mixtures, such emptying times were higher and for H2 mixture reached 25 s which, while close to the upper limit, was still considered satisfactory.

3.2. Assessment of mechanical properties

In order to obtain and compare the mechanical properties, the compressive strength, tensile splitting strength and modulus of elasticity were measured in accordance with the standards EN 12390-3 [47], EN 12390-6 [48] and ASTM ASTM: C469/C469 M. Three cylindrical specimens of each concrete type were tested for obtaining the compressive strength and tensile splitting strength. Modulus of elasticity was determined in one cylindrical specimen of each mixture. Table 3 shows the mean values and the coefficient of variation of the results. In Fig. 4, a mechanical properties variation of each FRC on the basis of the plain REF mixture is performed.

Table 3 shows that for medium fiber contents of both types of fibers, compressive strength slightly increased as compared with the reference concrete in accordance with some previous references as [21] or [34]. The compressive strength of P49 was similar to the reference concrete, while for P66, S33 and S49 it increased as may be seen in Fig. 4. It should be pointed out that all the mono-fiber mixtures had very close results to the REF mixture, at around 39 MPa. It is also noticeable that the addition of fibers did not imply compaction problems and that the results were similar in that they also had low dispersions.

Fig. 4 reveals that the compressive strength for hybrid mixtures decreased. As the volume fraction added was approximately doubled and the self-compacting properties decreased, such a change may be attributed to a worse compaction, what also coincides with previous research [21,32,34,38]. Through comparing hybrid fiber mixtures, it may be observed that the compressive strength was similar in both mixtures and close to 37 MPa which entailed a drop of 5%.

Fiber addition increased indirect tensile strength in all concretes. For REF mixture the tensile strength obtained was in the order of magnitude expected [2]. The best performance was obtained with the steel fibers that showed the best results, which was probably due to the anchorage of the fibers and the higher modulus of elasticity of the material itself. Moreover, the addition of polyolefin fiber also increased tensile strength.

Combination of the types of fibers provided similar results when both hybrid mixtures (H1 and H2) were compared. The result was 40% higher for the reference concrete and at values between the PFRC and SFRC (which was expected).

The reference concrete modulus of elasticity was close to 36GPa and decreased slightly for all concrete types with fibers. These results fitted those expected for PFRC, due to the lower modulus of elasticity of the fibers. In the case of steel fibers with a modulus of elasticity of six times higher when compared with concrete,

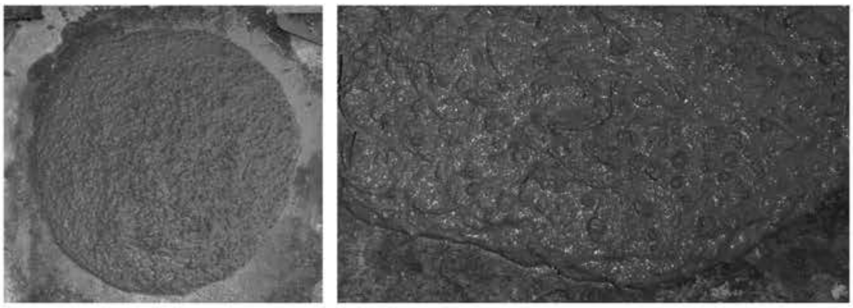

Fig. 3. Visual appearance of the slump-flow spread of H1.

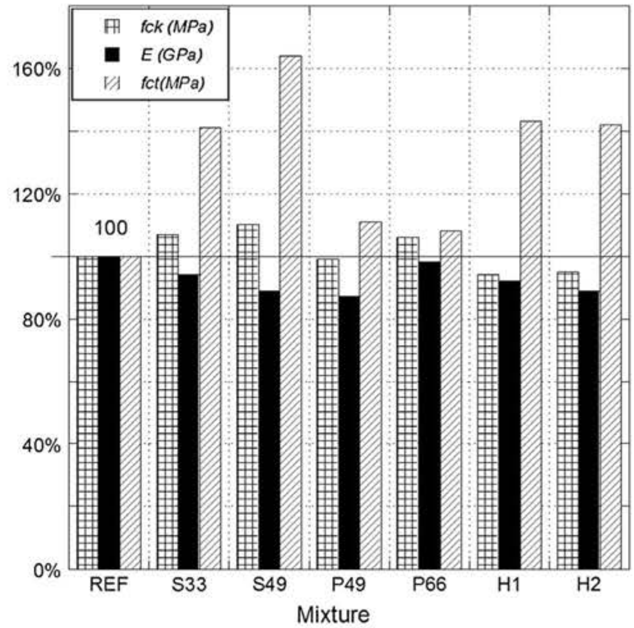

Fig. 4. Mechanical properties.

some other reasons such as a worse compaction (the SCC compaction was under its own weight, without vibration) might have caused the lower results of the composite material. Hybrid mixtures had similar values and were also in the gap of the results obtained for the conventional mono-fiber FRC mixtures.

3.3. Flexural tensile strength

3.3.1. Test setup

In accordance with RILEM TC-187-SOC [49] three-point bending tests were carried out in three prismatic specimens of each concrete type with dimensions $430 \times 100 \times 100\ \text{mm}^3$. The geometry was set based on the depth (D) of the sample shown in Fig. 5. Thus, span was chosen as three times the depth and the notch height as one third of the depth in the center of the span. The test was initially controlled by a clip-on gage crack mouth opening displacement (CMOD) device placed on the notch. Deflection was also measured by two linear variable differential transformer (LVDT) devices on each side of the specimen. Time, load and the machine actuator position data were also registered. When FRC deformations were higher than the upper limit of the CMOD device, the test control was changed to actuator position until the end of the test.

3.3.2. Test results and discussion

In order to obtain the fracture energy of each concrete, load–deflection curves and load–CMOD curves were assembled. As

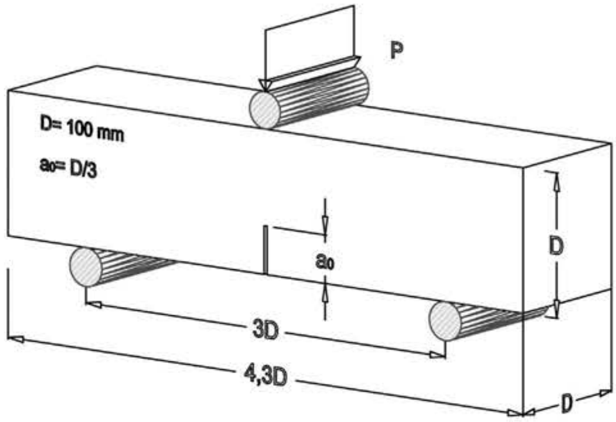

Fig. 5. Three-point bending test setup (mm).

previously mentioned, the load–CMOD curves registered values of only up to 4 mm. The comparable end of the test was defined at 8 mm of deflection. At that moment, no FRC specimens had collapsed. Three fracture tests were performed for every concrete mixture (Figs. 6 and 7 show the mean curves). Two main turning points of the curve shapes were also extracted (later discussed and shown in Table 4). The peak load (L_{PEAK}), defined as the first maximum load before the softening post-cracking branch and the minimum post-cracking load (L_{MIN}), were extracted. A summary of these values and the residual loads up to a CMOD of 0.5 mm, 1.5 mm, 2.5 mm and 3.5 mm extracted from load–CMOD curves, as well as the fracture energy results referring to deflection values of 1 mm, 5 mm and 8 mm determined from the load–deflection curves, are reported in Table 4.

A comparison of the experimental mean load–CMOD and load–deflection curves of the monotype FRC mixtures is shown in Fig. 6. The behavior of the reference concrete specimens was linear up to an elastic limit of about 50% of the peak load; from then on a deviation from linearity was observed due to the appearance and propagation of micro-cracks with the crack mouth width thus increasing faster. Once the peak load was reached, a clear softening branch followed until a quasi-brittle fracture occurred, dividing the specimens in two parts. The addition of a low fiber volume fraction of steel or polyolefin fibers enabled a ductile behavior. As the micro-cracks connected with each other and formed larger cracks, in addition to increasing the peak load, the fibers bridged more effectively both faces of the fracture surface which meant an improvement in the post-peak load bearing capacity and flexural toughness. When compared with the reference concrete specimens, as may be seen in Table 4, the higher the fiber volume content the better is the post-cracking response obtained.

SFRC specimens S33 and S49 showed increases in peak load of 20% and 16% respectively when compared with the reference

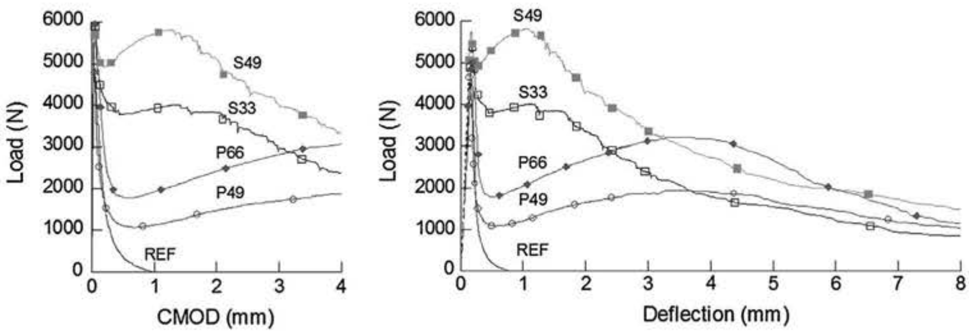

Fig. 6. Mean load–CMOD and load–deflection curves for monotype FRC mixtures.

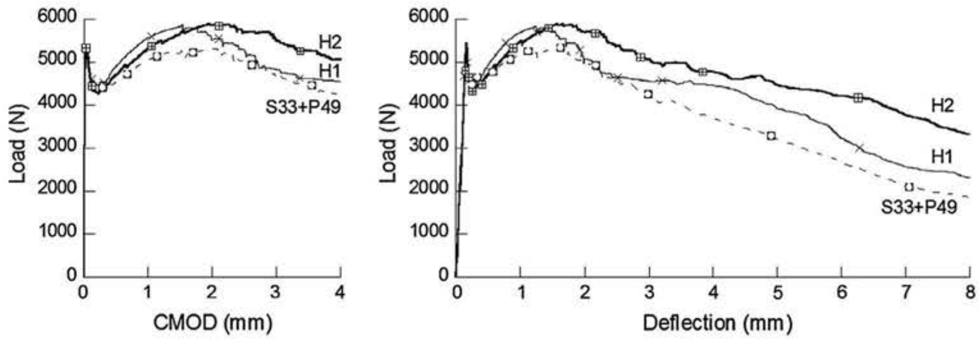

Fig. 7. Mean load–CMOD and load–deflection curves for hybrid FRC.

Table 4
Mean values of load and fracture energy (G_F) of concretes mixtures.

Concrete	L_{PEAK} (N)	c.v.	L_{MIN} (N)	c.v.	$L_{R0.5}$ (N)	c.v.	$L_{R1.5}$ (N)	c.v.	$L_{R2.5}$ (N)	c.v.	$L_{R3.5}$ (N)	c.v.	Fracture energy, G_F (N/m)		
													1 mm	5 mm	8 mm
REF	4970	0.04	–	–	–	–	–	–	–	–	–	–	130	–	–
S33	5975	0.06	3733	0.06	3764	0.05	3943	0.03	3406	0.06	2689	0.06	570	2135	2621
S49	5766	0.07	4900	0.16	5303	0.06	5660	0.09	4443	0.05	3732	0.10	752	2935	3759
P49	5655	0.01	1064	0.33	1131	0.31	1301	0.37	1640	0.38	1810	0.40	254	1292	1846
P66	6120	0.06	1754	0.23	1775	0.20	2142	0.26	2632	0.27	2999	0.26	347	2065	2769
H1	5412	0.03	4454	0.11	4893	0.08	5827	0.10	5294	0.07	4627	0.08	709	3577	4931
H2	5515	0.07	4287	0.07	4708	0.07	5650	0.04	5700	0.11	5266	0.12	679	3707	5583

concrete. S33 had almost constant residual loads of about 65% of peak load across the CMOD range of 0.5–1.5 mm. S49 exhibited a pseudo-hardening response as the steel fibers began to pull out from the matrix with residual loads of 92% and 98% of peak load in the same CMOD range. Then, as the hooked-end fibers with short embedded length were pulled out, a slight softening and descending branch took place until the end of the test in both concretes. These results dovetailed with previous research as Refs. [18] or [32].

PFRC specimens P49 and P66 showed an increment of the peak load of 14% and 23% respectively. In both concretes, after reaching the peak load, a steep descending branch began up to CMOD near 0.5 mm. At that point P66 showed a load decay of about 71%, while the P49 load was 81% of peak load. The residual loads increased substantially afterwards and almost linearly, recovering more than 49% of the peak load in concrete P66 and 32% of the peak load in concrete P49 at CMOD 3.5 mm. However, the highest residual loads were obtained from the load–deflection curves at deflection near 4 mm with values of 55% and 34% of their peak loads for P66 and P49 respectively. This indicates that polyolefin fibers at the used volumes require a considerable crack opening within the small displacement range (suffering the consequence of abrupt load decay after peak load) to improve the after-cracking behavior of the composite. The interlock between the fiber and the cracked matrix absorbs a considerable amount of energy in the large displacement range due to its moderate tensile strength and high elongation capacity. This post-cracking behavior was previously shown in Refs. [38] or [39] and subsequently expected.

If the results obtained from S49 and P49 (which had the same volume fraction content) are compared, the post-cracking strength and flexural toughness were higher in S49, due to steel fiber higher modulus and better anchorage with concrete matrix, as might have been expected. However, the absorption of energy performed by polyolefin fibers in large displacements was greater than that of steel fibers if fibers are compared weight for weight. For example, P66 with 6 kg/m^3 of polyolefin fibers had higher fracture energy than S33 with 26 kg/m^3 of steel fibers at a displacement value of 8 mm.

A comparison of mean load–CMOD and load–deflection curves between hybrid fiber-reinforced concretes H1 (0.33% SF + 0.49% PF) and H2 (0.25% SF + 0.66% PF) is shown in Fig. 7. The addition of flexural responses of both concretes S33 and P49 (with one type of fiber) resulted in a lower analytical curve compared with that experimentally obtained from H1. Therefore, a synergy effect between short hooked-end steel fibers and macro plastic polyolefin fibers led to an improved flexural tensile response of the hybrid-fiber

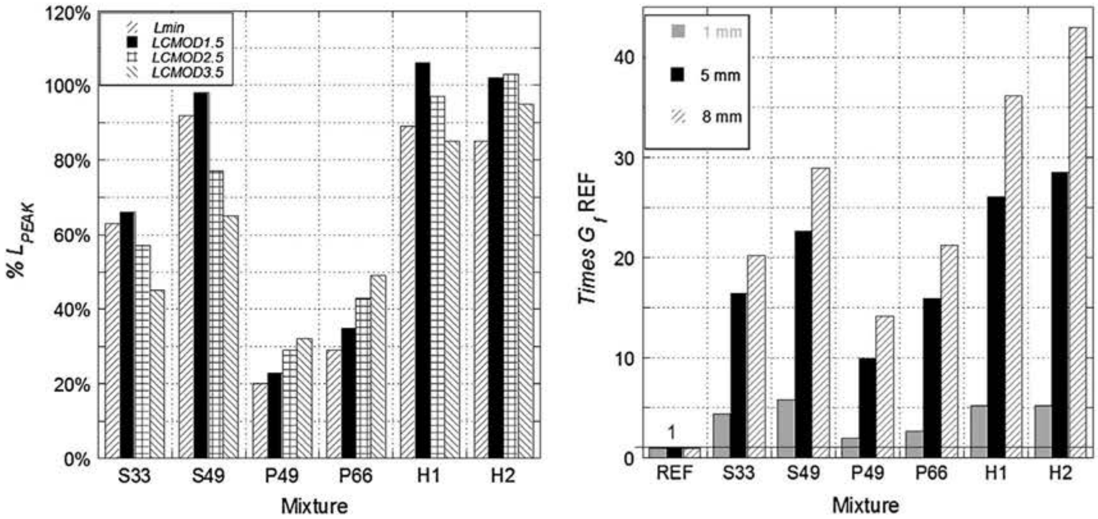

Fig. 8. Residual strengths and fracture energy.

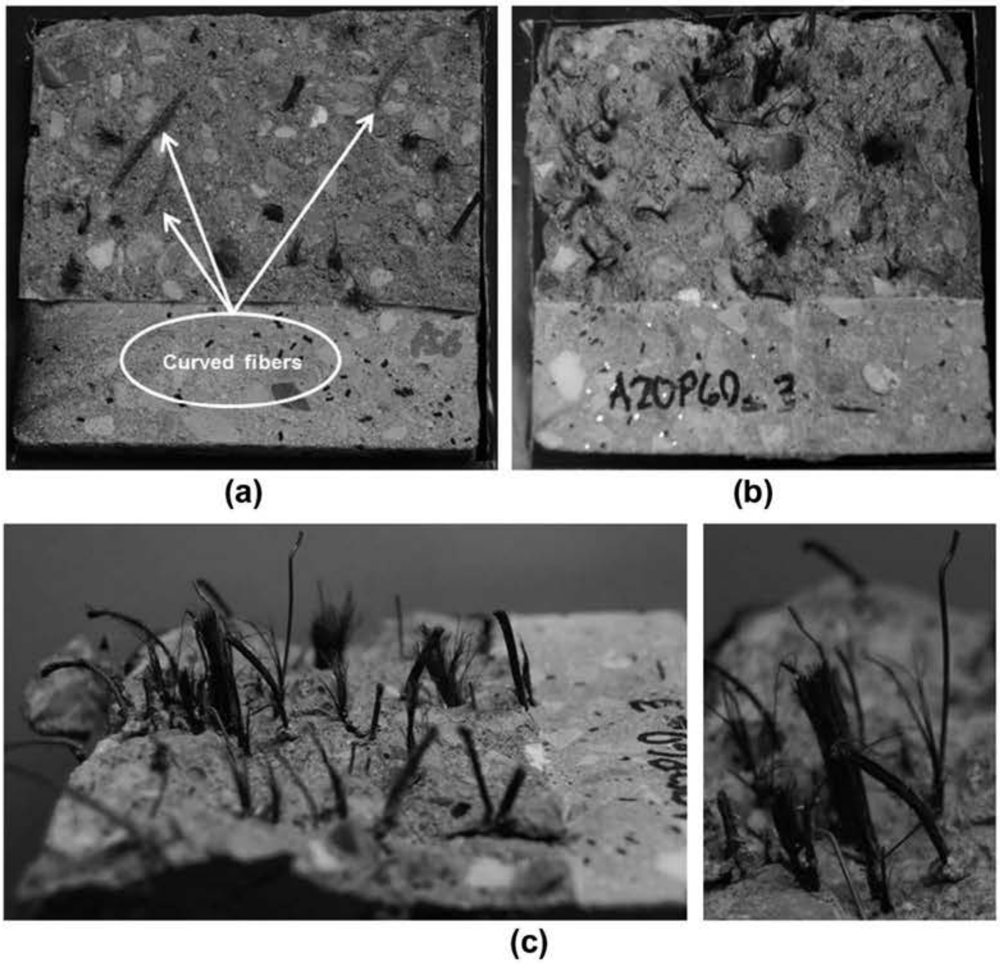

Fig. 9. Hybrid FRC improved fiber orientation of polyolefin fibers: (a) fracture surface of a P66 specimen; (b) fracture surface of a H2 specimen; (c) profile of a hybrid FRC (H2).

concretes. The mutual presence of the two types of fibers not only helped each fiber to mobilize more efficiently energy absorption capacity (obtaining residual loads in the first softening phase of 82% and 78% of the peak load in concrete H1 and H2 respectively), but also enabled a pronounced pseudo-hardening response and more stable post-cracking behavior compared with monotype FRC mixtures. Concrete H2, which had a total volume fraction of 1.11 times that of concrete H1, with 5 kg/m^3 less steel fiber and 1.5 kg/m^3 more polyolefin fiber, exhibited a better post-cracking response from CMOD 1.5 mm until the end of the test, showing higher flexural toughness than concrete H1.

Fig. 8 shows the relative residual loads in the specified CMOD values calculated as a percentage of the peak load of each mixture. The presence of two types of fibers in the hybrid concrete led to a more stable post-cracking behavior and higher residual values when compared with mono-fiber-reinforced concretes. Fig. 8 also shows the fracture energy of FRC mixtures in contrast to the fracture energy of the reference concrete in the specified deflection values. The fracture energy for a 5 mm and 8 mm deflection of hybrid composites is noticeably higher than for mono-fiber-reinforced concretes. Though the total fiber dosage of S49 (39 kg/m^3 of steel fibers) was higher than that of H1 (26 kg/m^3 SF + 4.5 kg/m^3 PF) and of H2 (20 kg/m^3 SF + 6 kg/m^3 PF), the residual loads of H1 and H2 were improved appreciably for CMOD greater than 1.5 mm.

As may be seen in Figs. 6–8, the combination of small amounts of hooked-end steel fibers with low and moderate volume fractions of polyolefin fibers (0.49% and 0.66%) provide the reference concrete matrix with a significant degree of energy absorption ability. These synthetic macro-plastic fibers give good energy absorption within the large displacement range, while the steel fibers improve residual load-bearing capacity in the small displacement range. Therefore, a material with a remarkable performance at low strains, which correlates with the serviceability limit state, was obtained. Moreover, this material showed stable post-cracking response and drastically improved fracture energy in the displacement values of 5 mm and 8 mm. These improvements were achieved, thus, using a low total content of fibers in weight.

3.3.3. Fracture surface analysis

The abovementioned synergy (shown in Fig. 7), with a rise in fracture results of H1 if compared with the sum of S33 and P49, suggested that the types of fibers interacted with each other, with the result being an enhancement of the composite properties. The reasons for this obtained extra rise could be explained by means of a fracture surface analysis. As previously shown, the post-cracking concrete behavior is closely linked with the number and distribution of fibers which is influenced by placing conditions as shown in Ref. [43]. In addition, it is known that steel fibers are rigid and tend to align with the flow of SCC, as previous research has shown, [31] though it should be noted that the low density and flexible nature of polyolefin fibers may cause a non-uniform distribution of the fibers.

In order to study the improvement achieved in the hybrid concretes, the fracture surfaces of all the concretes were analyzed. Specimens with only polyolefin fibers showed deficient orientation of the fibers as some were curved or even folded, as may be seen in Fig. 9(a). Furthermore, the distribution was not uniform on the fracture surface and contrary to what took place in the concretes with only steel fibers. Nonetheless, when hybrid FRC fracture surfaces were examined the orientation of both types of fibers seemed to be aligned with the same prevailing orientation, as may be seen in Fig. 9(b) and (c). The presence of the steel fibers may have oriented the polyolefin fibers, improving the fracture energy and load bearing capacities of H1 more than if the same amounts and types of fibers were added individually.

The theoretical number of fibers placed in the fracture surface was obtained for each concrete by using Eqs. (1) and (2), considering that the fibers were uniformly distributed and perpendicular to the crack.

$$V_f = \frac{W_f}{\rho \cdot V} \tag{1}$$

$$th = \frac{A \cdot V_f}{A_f} \tag{2}$$

In (1) and (2) V_f is the fiber volumetric fraction, W_f the weight of the fibers for a reference volume of 1 m^3, ρ the fiber density and V the total volume. In addition th is the theoretical number of fibers placed in the fracture surface of a given sample, with A being the cross section of the sample and A_f the section of one fiber. The average total number of fibers obtained from the counting exercise and its coefficient of variation (c.v.) is shown in Table 5. Moreover, the relation between the fibers counted in a given cross-section (n) and theoretical number of fibers (th) are shown in Table 5. This relation θ is the so-called in previous research [50] "orientation factor" or "fiber efficiency factor" that assumes a homogeneous distribution of fibers in the section and which may be seen in Eq. (3).

Table 5
Number of fibers on the fracture surface.

Concrete	# theoretical		# average total		c.v. (%)		θ	
	SF	PF	SF	PF	SF	PF	SF	PF
S33	139	–	94	–	14%	–	0.68	–
S49	208	–	104	–	2%	–	0.50	–
P49	–	74	–	45	–	13%	–	0.61
P66	–	99	–	64	–	28%	–	0.65
H1	139	74	104	47	4%	7%	0.75	0.63
H2	107	99	83	75	10%	16%	0.78	0.76

$$\theta = \frac{n}{th} = n\frac{A_f}{V_f A} \tag{3}$$

In the fracture surface analysis shown in Table 5, some observations regarding the counting process should be made. First of all, the steel fibers that appear in each half of the tested sample should be added because all of them were pulled-out. In relation to the polyolefin fibers, 79% were clearly broken and only 21% were pulled-out on average. Consequently, the total number of polyolefin fibers was obtained, in each sample, by adding the broken and the pulled-out fibers of the two fracture surfaces generated.

Regarding the distribution of fibers along the specimen, the coefficient of variation showed less scattering in the distribution of the steel fibers. The SCC flow showed good performance in spreading evenly the metallic rigid fibers. However, when polyolefin fibers were analyzed, the coefficient of variation rose up to 28% for P66 concrete. The use of a combination of steel and polyolefin fibers led to a sound improvement in terms of scatter when compared with the mixes manufactured only with polyolefin fibers. The lowest dispersion was found for the H1 mixture with coefficients of variation of 4% and 7% for steel and polyolefin fiber respectively.

On another note, if fibers were perfectly aligned, the number of fibers counted would match the theoretical value and, therefore, the ratio θ would be the unity. Consequently, the counting process supplies a value that deals with the orientation of the fibers. The values obtained for θ were remarkably higher for hybrid mixtures, as can be seen when comparing H1 with S33 and P49 and H2 with S49 and P66.

4. Conclusions

The development of polyolefin fibers with improved mechanical properties, in addition to surface treatments which enhance adhesion with matrix, both allow production of high-performance concretes with good ductility and flexural toughness. The polyolefin fibers are light and show a significant deformation capacity. The addition of a low amount of fibers enables a stable and reliable post-cracking behavior, maintaining fresh properties and with a lower weight of fibers.

It is possible to produce a hybrid fiber reinforced self-compacting concrete with a combination of hooked steel fibers and macro polyolefin fibers, preserving the high performance fresh properties within the most common self-compacting requirements. It should also be noted that the addition of fibers did not noticeably change the compressive strength, indirect tensile strength or modulus of elasticity of the reference SCC for any of the amounts, types or combination of fibers used.

It was possible to make a polyolefin fiber-reinforced concrete improved with the addition of low amounts (20–26 kg/m^3) of steel-hooked fibers. The fracture toughness and ductility, as well as residual strength, were increased if compared with the same proportions added separately and subsequently combined. This synergy in the fracture results led to a high-performance concrete capable of bearing loads close to the peak-load for deflections of L/60.

The weak point of polyolefin fiber-reinforced concrete for structural design, it could be argued, might be for small deflections. It is possible to produce a concrete with an almost constant post-cracking load bearing capacity by adding steel fibers to the fiber cocktail in the case of structural use being demanded. This paper suggests that it could be possible to produce a hybrid fiber-reinforced concrete with a fiber cocktail made of steel-hooked fibers and macro polyolefin fibers with a bilinear fracture load–deflection behavior. The combination of the two types of anchorage chosen, it would seem, could offer a suitable joint action.

The combination of stiff and heavy fiber with a low density flexible synthetic macro fiber showed an additional advantage that enhances the orientation of the polyolefin fibers. The steel fibers enhanced the alignment of the polyolefin fibers, tending to place both types of fibers with the preferential orientation of the flow of self-compacting concrete. This improving effect was observed on the fracture surface of the specimens that showed the same preferential orientation for both types of fibers and a more uniform distribution of the polyolefin fibers.

Acknowledgements

The authors gratefully acknowledge the financial support provided by Ministry of Economy and Competitiveness of Spain by means of the Research Fund Project PDI 2011-24876. They also offer their gratitude to SIKA SAU for supplying the polyolefin fibers. Marcos García Alberti also wishes to express his gratitude to SIKA SAU for the grant provided.

References

Parra C, Valcuende M, Gómez F. Splitting tensile strength and modulus of elasticity of self-compacting concrete. Constr Build Mater 2011;25(1):201–7.
Almeida Filho FM, Barragán BE, Casas JR, El Debs ALHC. Hardened properties of self-compacting concrete – a statistical approach. Constr Build Mater 2010;24(9):1608–15.
Domone P. Self-compacting concrete: an analysis of 11 years of cases studies. Cem Concr Compos 2006;28(2):197–208.
Bissonnette B, Pierre P, Pigeon M. Influence of key parameters on drying shrinkage of cementitious materials. Cem Concr Res 1999;29:1655–62.
Banthia N, Gupta R. Influence of polypropylene fiber geometry on plastic shrinkage cracking in concrete. Cem Concr Res 2006;36(7):1263–7.
Shah S, Rangan B. Fiber reinforced concrete properties. J Am Concr Inst 1971;68(2):126–35.
Brandt A. Fibre reinforced cement-based (FRC) composites after over 40 years of development in building and civil engineering. Compos Struct 2008;86(1–3):3–9.
Ivorra S, Garcés P, Catalá G, Andión LG, Zornoza E. Effect of silica fume particle size on mechanical properties of short carbon fiber reinforced concrete. Mater Des 2010;31(3):1553–8.
Aveston J, Cooper G, Kelly A. In: the properties of fiber composites, de Conference proceedings. IPC, Science and Technology; 1971.
Prisco Md, Lamperti M, Lapolla S Khurana R. HPFRCC thin plates for precast roofing, de Proceedings of second international symposium on ultra high performance concrete. Kassel; 2008.
Caverzan A, Cadoni E, Di Prisco M. Dynamic tensile behavior of self-compacting steel fibre reinforced concrete. Appl Mech Mater 2011;82:220–5.
Lok TS, Zhao PJ. Impact response of steel fiber-reinforced concrete using a split Hopkinson pressure bar. J Mater Civil Eng 2004:54–9.
Goel S, Singh SP, Singh P. Flexural fatigue strength and failure probability of self compacting fibre reinforced concrete beams. Eng Struct 2012;40:131–40.
Jean-Louis Granju SUB. Corrosion of steel fibre reinforced concrete from the cracks. Cem Concr Res 2005;35(3):572–7.
ACI Committee 544, ACI 544. 1R-96.State-of-the-art report on fiber reinforced concrete, reapproved; 2009.
El-Dieb AS. Mechanical, durability and microstructural characteristics of ultra-high-strength self-compacting concrete incorporating steel fibers. Mater Des 2009;30(10):4286–92.
Park SH, Kim DJ, Ryu GS, Koh KT. Tensile behavior of ultra high performance hybrid fiber reinforced concrete. Cem Concr Compos 2012;234(2):172–84.
Holschemacher K, Mueller T, Ribakov Y. Effect of steel fibres on mechanical properties of high-strength concrete. Mater Des 2010;31(5):2604–15.
Vandewalle L. Hybrid fibre concrete: is there a synergetic effect? In: Adv Constr Mater. Berlin (Heidelberg): Springer; 2007. p. 219–28.
Aydin AC. Self compactability of high volume hybrid fiber reinforced concrete. Constr Build Mater 2007;21(6):1149–54.
Yao W, Li J, Wu Keru. Mechanical properties of hybrid fiber-reinforced concrete at low fiber volume fraction. Cem Concrte Res 2003;33(1):27–30.
Skazlic M, Bjegovic D. Effects of hybrid fibres on the properties of fiber-reinforced concrete. In: the proceedings of: 6th international RILEM symposium on fibre reinforced concretes, Eds. di Prisco M, Felicetti R, Plizzari GA, Varenna (Italy); 2004.
Vandewalle L. Hybrid fiber reinforced concrete. In: Measuring, monitoring and modeling concrete properties. Netherlands: Springer; 2006. p. 77–82.
Wang P, Huang Z, Jiang J, Wu Y. Performance of hybrid fiber reinforced concrete with steel fibers and polypropylene fibers. Civil Eng Urban Plan 2012;2012:458–61.
Qiany C, Stroeven P. Fracture properties of concrete reinforced with steel–polypropylene hybrid fibres. Cem Concr Compos 2000;22(5):343–51.
Qiany C, Stroeven P. Development of hybrid polypropylene–steel fibre-reinforced concrete. Cem Concr Res 2000;30(1):63–9.
Komloš K, Babál B, Nürnbergerová T. Hybrid fibre-reinforced concrete under repeated loading. Nucl Eng Des 1995;156(1-2):195–200.
Sonebi M. Medium strength self-compacting concrete containing fly ash: modelling using factorial experimental plans. Cem Concr Res 2004;34(7):1199–208.
Sahmaran M, Yurtseven A, Yaman IO. Workability of hybrid fiber reinforced self-compacting concrete. Build Environ 2005;40(2):1672–7.
Burcu Akcay MAT. Mechanical behaviour and fibre dispersion of hybrid steel fibre reinforced self-compacting concrete. Constr Build Mater 2012;28(1):287–93.
Stähli P, Custer R, Mier JGM. On flow properties, fibre distribution, fibre orientation and flexural behaviour of FRC. Mater Struct 2007;41(1):189–96.
Pająk M, Ponikiewski T. Flexural behavior of self-compacting concrete reinforced with different types of steel fibers. Constr Build Mater 2013;47:397–408.
Ding Y, Liu S, Zhang Y, Thomas A. The investigation on the workability of fibre cocktail reinforced self-compacting high performance concrete. Constr Build Mater 2008;22(7):1462–70.
Ding Y, Zhang Y, Thomas A. The investigation on strength and flexural toughness of fibre cocktail reinforced self-compacting high performance concrete. Constr Build Mater 2009;23(1):448–52.
Dawood ET, Ramli M. Mechanical properties of high strength flowing concrete with hybrid fibers. Constr Build Mater 2012;28(1):193–200.
You Z, Chen X, Dong S. Ductility and strength of hybrid fiber reinforced self-consolidating concrete beam with low reinforcement ratios. Syst Eng Proc 2011;1:28–34.
Ganesan N, Indira PV, Sabeena MV. Behaviour of hybrid fibre reinforced concrete beam–column joints under reverse cyclic loads. Mater Des 2014;54:686–93.
Alberti MG, Enfedaque A, Gálvez JC. On the mechanical properties and fracture behavior of polyolefin fiber-reinforced self-compacting concrete. Constr Build Mater 2014;55(31):274–88.
Behfarnia K, Behravan A. Application of high performance polypropylene fibers in concrete lining of water tunnels. Mater Des 2014;55:274–9.
Han T-Y, Lin W-T, Cheng A, Huang R, Huang C-C. Influence of polyolefin fibers on the engineering properties of cement-based composites containing silica fume. Mater Des 2012;37:569–76.
Buratti N, Mazzotti C, Savoia M. Post-cracking behaviour of steel and macro-synthetic fibre-reinforced concretes. Constr Build Mater 2011;25(5):2713–22.
Oh BH, Kim JC, Choi YC. Fracture behavior of concrete members reinforced with structural synthetic fibers. Eng Fracture Mech 2007;74(1-2):243–57.
Zerbino R, Tobes JM, Bossio ME, Giaccio G. On the orientation of fibres in structural members fabricated with self compacting fibre reinforced concrete. Cem Concr Compos 2012;34(2):191–200.
EN 12350-8:2010. Testing fresh concrete. Part 8: self-compacting concrete. Slump-flow test; 2010.
EN 12350-9:2010. Testing fresh concrete. Part 9: self-compacting concrete. V-funnel test; 2010.
Walraven J. Structural application of self compacting concrete, from Proceedings of 3rd RILEM international symposium on self compacting concrete, Reykjavic, Iceland; 2003.
EN 12390-3:2009. Testing hardened concrete. Part 3: compressive strength of test specimens; 2009.
EN 12390-6:2009. Testing hardened concrete. Part 6: tensile spliting strength of test specimens; 2009.
RILEM, TC-187-SOC.Indirect test for stress-crack opening curve; 2007.
Martinie L, Roussel N. Simple tools for fiber orientation prediction in industrial practice. Cem Concr Res 2011;41(10):993–1000.